Electron ionization of bare neon clusters and neon clusters doped with CO_2 molecules

Georg Alexander Holzer,[1] Rebecca Meißner,[1,2] Anita Ribar,[1] Andreas Bayer,[1] Michael Neustetter,[1] and Stephan Denifl[1,*]

[1]*Institut für Ionenphysik und Angewandte Physik, Universität Innsbruck, Technikerstrasse 25, A-6020, Innsbruck, Austria*

[2]*Atomic and Molecular Collisions Laboratory, CEFITEC, Department of Physics, Universidade NOVA de Lisboa, 2829-516, Caparica, Portugal*

(Received 4 February 2020; accepted 3 April 2020; published 28 April 2020)

In the present study we have investigated the ionization threshold behavior of neon cluster ions Ne^{n+} (with $n = 2-6$) formed upon the electron ionization of small neon clusters. The clusters were formed by supersonic expansion of cold neon gas through a pinhole nozzle. The appearance energies for these cluster ions were subsequently determined using a nonlinear least-squares fitting procedure. The obtained thresholds turned out to be only slightly lower than the ionization energy of the single neon atom. The present results are compared with previous electron impact and photoionization results. In addition, we investigated the electron ionization of neon clusters doped with CO_2 molecules. The mass spectrum at the electron energy of 70 eV showed predominantly bare cluster ions of CO_2. Charged clusters with fragments of CO_2 were observed as well, though in weaker abundance than the intact cluster ions. The relative abundance of these fragment ions was different from the ratios previously reported for electron ionization of bare CO_2 clusters and indicated increased formation of $(CO_2)_4O_2^+$ due to a neon matrix effect. We further investigated the ionization mechanisms in the cluster by measuring the ion yields of $(CO_2)_4^+$ as a function of the electron energy close to the threshold. Direct ionization by the incoming electron, Penning ionization, and charge-transfer ionization were identified as possible processes, with varying contributions for different initial mean neon cluster sizes.

DOI: 10.1103/PhysRevA.101.042708

I. INTRODUCTION

Neon clusters have a particular position in the group of rare gas clusters, since they are the intermediate species between the fully liquid helium clusters and the solid clusters of the heavier rare gases argon, krypton, and xenon. Though different phases are ascribed to the neutral clusters, magic numbers appeared in the mass spectrum of all rare gas clusters upon ionization by electrons. Those magic numbers can be viewed as a distinct property of a solid cluster [1,2]. Magic numbers turned out to be common for rare gases such as for cluster sizes $n = 13$ and 55 related to an icosahedral structure, but Märk and Scheier also proposed specific numbers like $n = 21$ and 75 for neon clusters [3]. The same authors also reported an isotope effect in clustering of neon, which led to an enrichment of heavier isotopes in neon clusters [4]. This effect can be explained by isotope-dependent reaction rates in the processes during the cluster growth, which result from the slightly different zero-point energies, depending on whether the lighter Ne-20 isotope is involved or the heavier Ne-22 (the Ne-21 isotope was neglected due to its low abundance of 0.27%) [4,5]. However, Fieber *et al.*, who studied photoionization of small neon clusters, ascribed the effect also to the fragmentation process after the ionization [6]. Electron ionization mass spectra for isotopically pure Ne-20 gas further allowed determination of the critical cluster sizes for the detection of doubly and triply charged neon clusters [7].

For the measurement of mass spectra a fixed electron energy is chosen where the ion yield has its maximum. The appearance energy (AE) of a mass selected cluster ion is another important quantity, which is typically determined by collecting the ion yield of a mass selected cluster while the kinetic energy of the incoming electron is varied. One major result of previous electron ionization as well as photoionization studies was that yields of rare gas cluster ions can also be observed below the ionization energy of the single atom [6,8,9]. Though those ion yields turned out to be weak compared to the maximum yields obtainable above the atomic ionization threshold, they raised particular interest, since other ionization mechanisms (like autoionization) must be operative compared to direct ionization.

More information about possible ionization mechanisms and general properties of clusters can be gained by studying doped clusters. Such studies were carried out so far particularly with helium droplets [1,10], employing the well-known pickup technique to generate doped droplets. The subsequent localization of dopants in the helium droplets is well studied and can be predicted by the Ancilotto parameter [11]. The helium matrix allows formation of cold, novel species due to its unique superfluidity at 0.37 K [1]. Neon clusters formed by evaporative cooling during supersonic expansion are slightly warmer, providing a temperature of 10 K [12]. As will be shown in the present study, this heat bath is still sufficient for the formation of small dopant clusters. Several studies provided information about the localization of dopants in neon clusters with different sizes [13–20]. In particular, phase transitions from fluid to solid were predicted at the size of

*Corresponding author: stephan.denifl@uibk.ac.at

$N \geqslant 300$, which will influence the localization of dopants [21]. In the case of solid clusters, dopants favor surface states [13–17], which is characteristic for argon clusters [22–25].

In the present study, we investigated pure and doped neon clusters ionized by electron ionization. In the case of pure clusters, we have measured the ion yield close to the threshold for Ne^{n+} with $n = 2-6$ and determined the corresponding AEs. As discussed below in the Results and Discussion section, the adiabatic ionization energy of the neon dimer cannot be reached in electron ionization experiments employing supersonic expansion for generation of clusters. In another set of measurements, we have also doped the neon clusters with carbon dioxide before electron ionization. Subsequently, we measured ion efficiency curves close to the threshold for resulting dopant ions. These ion yield curves provide evidence on the underlying ionization mechanism, as well as information on the initial localization of the dopant in an interior or exterior state [26]. Another important general question in the study of dopants concerns the modification of the fragmentation process by the presence of a surrounding matrix, which acts as a heat bath [27]. Electron ionization at the electron energy of about 70 eV may lead to dissociation of molecules, which may be quenched by energy dissipation into the cluster environment. In order to investigate this process in the case of doped neon clusters, we recorded the mass spectrum of the doped cluster at an electron energy of 70 eV.

II. EXPERIMENTAL SETUP AND DATA ANALYSIS

The experimental device utilized for the present study consisted of a modified cluster source based on a previous design and a high-resolution hemispherical electron monochromator coupled with a quadrupole mass spectrometer (for more details see [28]). Neutral clusters were generated by supersonic expansion of neon at different expansion pressures and temperatures through a 10-μm nozzle. The mean cluster size of the neutral neon clusters $\langle N \rangle$ was estimated by using empirical equations introduced in Ref. [29]. The cluster source was mounted on a closed-cycle helium cryostat which allowed cooling of the gas to the required temperatures. A silicon diode and a resistive heater, which were connected to a temperature controller, were used to measure and control the cluster source temperature. The background pressure in the chamber containing the cluster source (as well as in the subsequently attached chambers) was in the order of 10^{-8} mbar. During the neon expansion this pressure raised to about 2×10^{-4} mbar.

After a distance of about 1 cm from the nozzle, the cluster beam passed a conical skimmer of 1 mm diameter before entering a pickup stage, which had a length of about 15 cm. In the case of pickup experiments, CO_2 was introduced into this stage by a leak valve. The working pressure adjusted for pickup was $\sim 8 \times 10^{-4}$ mbar. For the investigations with pure clusters the valve remained closed. The cluster beam entered the chamber with the monochromator through a hole (opening diameter 1 mm) of a plate which separated the pickup stage and monochromator stage. The cluster beam crossed an electron beam in the hemispherical electron monochromator (HEM). The homemade HEM generated an electron beam emitted from a tungsten hairpin filament with an electron current in the order of few tens of nanoamperes. The electron-beam resolution was $\sim$100 meV in the course of the present measurements. The linearity of the energy scale and the width of the energy distribution were proven in several previous studies. The systematic error of the energy scale was determined to be less than 10 meV in the energy range from about zero to 60 eV [30,31]. Such accuracy over this extended energy scale is of great importance for the present experiment, as neon has a much higher ionization energy than carbon dioxide (see the next section). The threshold of the monomer was used for the calibration of the electron energy scale. Cations formed in the interaction of the monochromatized electron beam and the cluster beam were subsequently extracted by a weak electrostatic field towards the entrance of the quadrupole mass spectrometer (mass range 1–2048 u). The mass selected cations were bent off axis by two deflectors and finally detected by a channeltron-type secondary electron multiplier. Mass spectra were recorded at a fixed electron energy of about 70 eV, while the threshold behavior of a mass selected cation was measured by setting the quadrupole to its corresponding mass and scanning the electron energy in the range of a few electronvolts below and above the threshold. The detected ion signal was processed by a computer.

For the determination of the AE of a certain cation we utilized a nonlinear least-squares fitting routine using the Marquart-Levenberg algorithm. The measured ionization efficiency curve was fitted with the following function $f(E)$ [32]:

$$f(E) = b \quad \text{for} \quad E < AE_1, \tag{1a}$$

$$f(E) = b + c(E - AE_1)^{p_1} \quad \text{for} \quad AE_1 < E < AE_2, \tag{1b}$$

$$f(E) = b + c(E - AE_1)^{p_1} + d(E - AE_2)^{p_2} \quad \text{for} \quad E > AE_2. \tag{1c}$$

This function resembles a threshold law of exponential type, which is based on the theory by Wannier [33]. Then the fit for function (1b) comprises four parameters: a background signal b, a scaling constant c, which is zero in Eq. (1a) (corresponding to the ion yield below the threshold), the appearance energy AE_1, and the exponent p_1. For ionization efficiency curves, which exhibited a second threshold (for example, due to a different ionization mechanism or a different ionic state or a second process, which leads to the ion with the same mass), function (1b) was extended by a third term, as shown in function (1c). AE_2 is then the corresponding AE of the second threshold and p_2 the second exponent.

In addition, the fit function was folded with a Gaussian distribution $g(E)$ to include the finite resolution of the electron energy beam. Mathematically this can be expressed by a function $h(E)$ with

$$h(E) = \int f(E) * g(E) dE. \tag{2}$$

The fitting of the data was performed with MATCAD. With this fitting method a reliable and reproducible determination of appearance energies can be achieved, which was demonstrated previously for different molecules [32,34].

For the determination of AEs for cluster ions resulting from ionization of neon clusters doped with CO_2 we uitilized a more recent fitting program written in PYTHON. This program

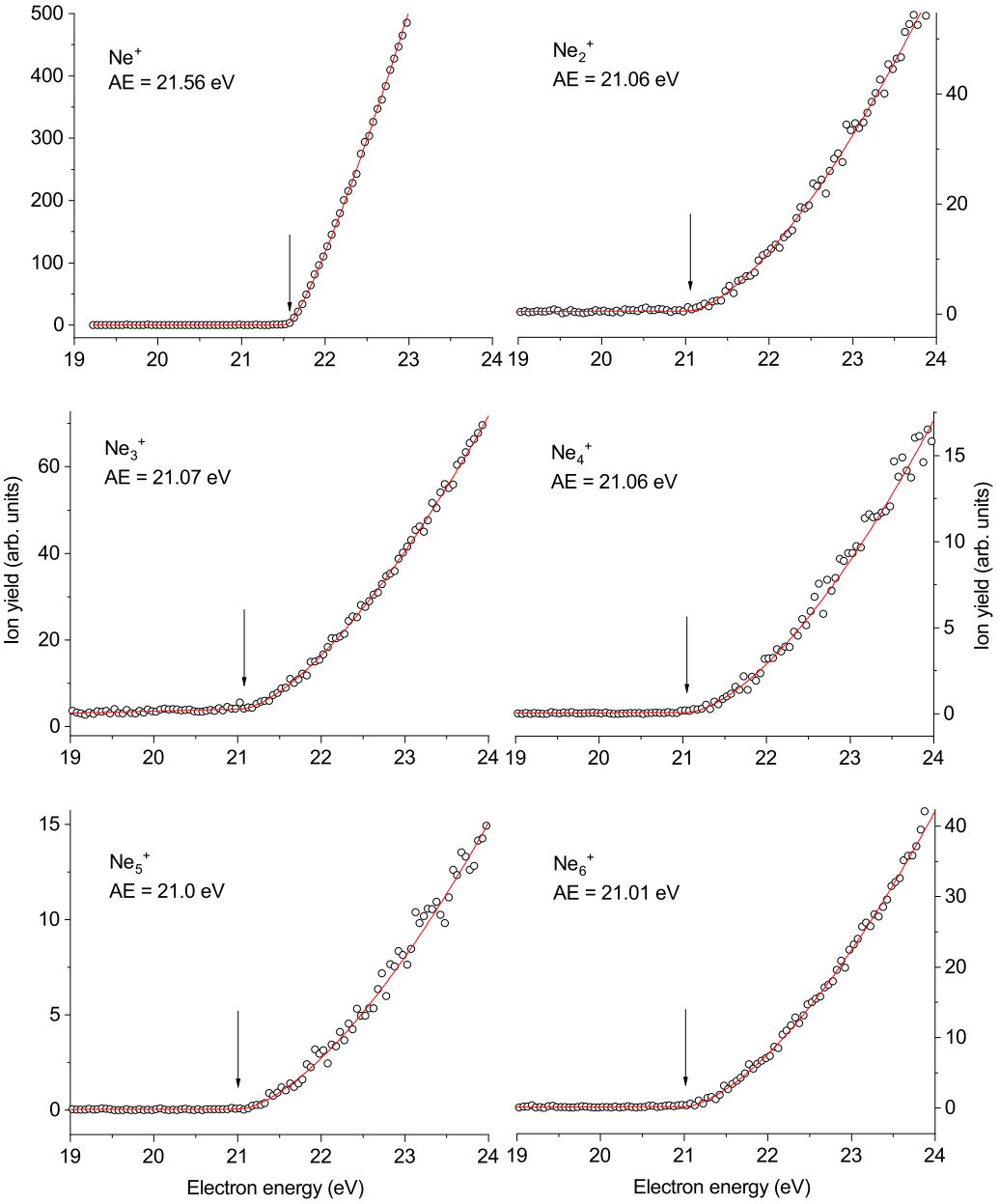

FIG. 1. Threshold ionization efficiency curves (open circles) of small neon cluster ions Ne^{n+} for $n = 2-6$. The corresponding measurement of atomic Ne^+, which was used to calibrate the electron energy scale, is also included in the figure. The fit curves are shown as solid lines. The arrows indicate the derived thresholds.

is based on the Wannier function as well and also includes the finite resolution of the electron energy beam. Compared to the fitting program in MATCAD, the PYTHON fitting routine was faster, which was favorable if a scan showed multiple thresholds. For a more detailed description of the PYTHON fitting routine we refer to [35].

III. RESULTS AND DISCUSSION

A. Ionization of pure neon clusters

Figure 1 shows ion efficiency curves close to the threshold for the Ne^+ ion (monomer) and small neon cluster ions Ne^{n+} for $n = 2-6$. The nozzle temperature was 90 K and the neon pressure 13 bar. The corresponding mean size of neutral clusters is $\langle N \rangle \sim 16$ for these expansion conditions. The ion efficiency curve close to the threshold for the monomer (atomic neon) shows just a single threshold, as expected. We just note that in a previous study of helium clusters using the same crossed beam setup, the ion yield of the helium monomer showed a first threshold at 21.29 eV, which is below the atomic ionization energy of helium (24.56 eV) [8]. This threshold was finally ascribed—after a sequence of additional studies–to the initial formation of the electronically excited helium anion He^{*-} which interacts with a He* atom in the droplet and forms $He^+ + He + 2e^-$ [36].

The AEs derived with the fitting method introduced above are listed in Table I. The value for the monomer, which corresponds to the ionization energy (IE) of the neon atom

TABLE I. Appearance energies of small neon cluster ions Ne_n^+ up to cluster size $n = 6$ formed upon electron ionization of bare neon clusters. The present values are compared with values from previous electron ionization and photon ionization studies.

	Appearance energy of Ne_n^+ (in eV)				
Cluster size n	Present work	Fiegele [a]	Munson *et al.*[c]	Hall *et al.*[d]	Trevor *et al.*[e]
2	21.06 ± 0.07	21.004–20.65[b]	20.9 ± 0.2	20.411 ± 0.01	20.33 ± 0.08
3	21.07 ± 0.04	21.028			
4	21.06 ± 0.09	21.048			
5	21.0 ± 0.1	21.048			
6	21.01 ± 0.05	21.039			

[a]Electron ionization value taken from Ref. [41].
[b]Values for range of different expansion conditions (see text).
[c]Electron ionization value taken from Ref. [42].
[d]Photon ionization value taken from Ref. [43].
[e]Photon ionization value taken from Ref. [44].

(21.564 eV [30,37]), was used for calibration of the electron energy scale and is listed for comparison. All investigated neon cluster ions show a lower AE than the IE of neon. The value ranges from 21.06 ± 0.07 eV for Ne_2^+ down to 21.01 ± 0.05 eV for Ne_6^+. Taking into account the error margins included in Table I, the AEs are very similar for the investigated range of cluster sizes and are about 0.5 eV lower than the IE for atomic neon. The general tendency of a lower AE of cluster ions compared to the ionization energy of the monomer has been previously observed for rare gas clusters like argon [9] and helium [8] and can be well understood by the consideration of the potential energy of the neutral and positively charged neon dimer as a function of the internuclear distance. A figure of the corresponding potential energy surfaces can be found in Ref. [38]. As the figure reveals, a strong change of the geometry occurs upon the ionization of the dimer. The electronic ground state of neutral Ne_2 has a very shallow minimum at about 3.2 Å [38] with a dissociation energy of 3.5 meV [39]. For the positively charged neon dimer in its electronic $1\,^2\Sigma_u^+$ ground state, the equilibrium distance is shortened to 1.72 Å along with an increase of the dissociation energy to 1.283 eV [40]. Knowing these parameters, the adiabatic ionization energy (AIE) of the neon dimer can be calculated by the following formula:

$$\mathrm{AIE}(Ne_2^+/Ne_2) = \mathrm{IE}\left(Ne^+/Ne\right) + D(Ne - Ne) - D(Ne^+ - Ne), \quad (3)$$

with D as the corresponding dissociation energies of the neutral neon dimer and the neon dimer cation. Equation (3) yields an AIE of 20.285 eV for the neon dimer, which is about 0.8 eV lower than the presently obtained AE. Such an AE value between the AIE of the dimer and the IE of the monomer may indicate that a vertical Franck-Condon transition into the outer region of the potential well of Ne_2^+ occurs. However, the results of another electron ionization study of small neon clusters by Fiegele [41] may provide a more likely explanation. The AEs by Fiegele are also included in Table I. No error margins for the derived AE values have been reported in his thesis [41], and the finite resolution of the electron beam was not taken into account in the fitting procedure. However, the tendency of a lower AE of neon clusters compared to the monomer seems to be in line with the present results. Moreover, Fiegele determined the AE of the neon dimer cation for different expansion conditions. The nozzle temperature was varied between 70 and 120 K, and

TABLE II. Appearance energies of $(CO_2)_4^+$ formed upon electron ionization of neon clusters doped with CO_2, measured at different temperatures of the nozzle. The present values are compared with relevant literature values.

Appearance energies of $(CO_2)_4^+$ (in eV)					
Nozzle temperature			Bare CO_2 clusters[a]	Threshold of Ne∗[b]	Threshold of Ne^+[c]
100 K	75 K	65 K			
13.61 ± 0.09	13.91 ± 0.09		12.6 ± 0.1		
15.80 ± 0.11					
	16.60 ± 0.07	16.1 ± 2.9		16.619 ($3s\,^3P_2$)	
	17.31 ± 0.02				
	18.5 ± 0.1	18.8 ± 0.6		18.382 ($3p\,^3S_1$)	
	21.47 ± 0.07	21.7 ± 0.2			21.56

[a]Value taken from Ref. [58].
[b]Values taken from Ref. [66].
[c]Value taken from Ref. [37].

he observed a decrease of the AE for warmer expansion conditions. Such behavior was also found for small argon clusters [9]. For mild expansion conditions—high nozzle temperature and low expansion pressure—clustering is weak and the cluster beam contains predominantly only dimers. In such cases the dimer ion can only result from ionization of the neutral dimer. In contrast, the predominant source of the dimer ion at colder conditions are larger clusters which fragment upon the ionization. The presently chosen expansion conditions with $\langle N \rangle \sim 16$ would clearly allow the formation of the dimer ions upon dissociative electron ionization of slightly larger clusters. This would also explain the similar AEs found for the other cluster sizes. The AE value of the neon dimer ion formed upon electron impact was also reported by Munson *et al.* (20.9 ± 0.2 eV) [42]. They utilized a magnetic sector as a mass analyzer and a standard electron source without monochromatizing element. Moreover, no supersonic expansion was used to generate dimers; instead, electron ionization in a high-pressure environment was studied, which should rule out formation of larger clusters. However, the production of the charged dimer resulted rather from chemical ionization reactions than direct electron impact. The measured ion yield of the dimer cation showed typical characteristics that ions are formed via electronically excited states. Hence, it was concluded that the dimer cation is formed upon the collision of an electronically excited monomer with another monomer in the ground state [42].

A substantially lower AE of the dimer cation was obtained in photoionization experiments [43,44]. Hall *et al.* generated neon dimers in a supersonic expansion at mild conditions (300 K, 1 bar, nozzle diameter 30 μm) and obtained a photoionization threshold of 20.411 ± 0.01 eV [43]. In agreement, Trevor *et al.* obtained the AE of 20.33 ± 0.08 eV upon the photoionization of the neutral dimer (77 K, 2.66 bar, nozzle diameter 20 μm) [44]. These AE values from the photoionization experiments are closer to the calculated AIE of 20.285 eV derived above than the electron ionization values. Since it is impossible in an ionization event of a cluster that this AIE can be reached experimentally by a vertical Franck-Condon transition, autoionization via high-lying Rydberg states of the neutral was proposed as mechanism for photoionization below the IE of the neon atom [44]. In contrast, the signature of such autoionization processes of the neon dimer become masked in the electron ionization studies of small neon clusters, due to the fragmentation of larger clusters, as discussed above. Moreover, we note that the present AE values are below the vertical ionization energy (VIE) of 21.39 eV derived in semi-empirical calculations by Chen *et al.* [45]. The deviation of up to ~0.4 eV may be explained by the fact that the Franck-Condon overlap between initial state and final state has its maximum at the VIE; however, vertical transitions are also possible at somewhat lower energies [9]. More recent theoretical calculations for argon clusters indicated that AEs below the VIE may also be explained by nuclear delocalization effects [46], where thermal excitations or zero-point vibrations of the floppy clusters lead to a red-shift of predicted vertical appearance energies. We just note that nuclear quantum effects were studied for neon cluster ions as well [47]. It was predicted that those effects play an important role for the formation of magic numbers like

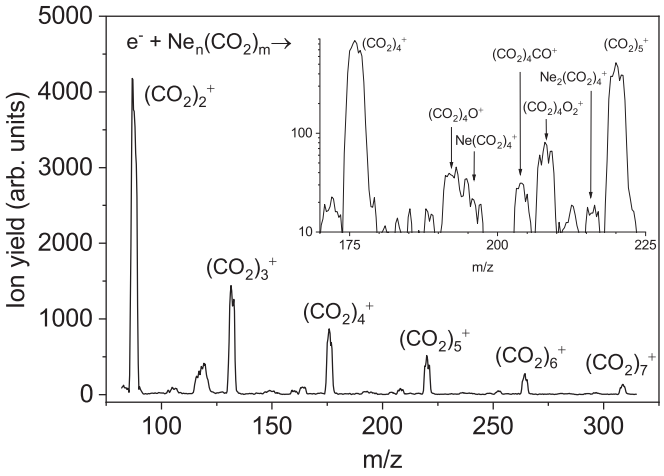

FIG. 2. Resulting electron ionization mass spectrum for neon clusters doped with CO_2, in the m/z range from 81 to 314. The spectrum was recorded at the initial electron energy of 70 eV. The inset shows a detailed view of the same spectrum in the mass range between m/z 170 and m/z 225.

$n = 14$ and $n = 56$, since for those particular sizes, as well as for the trimer, energy fluctuations are minimized. Moreover, an ionic dimer core was modeled for small cluster ions [47,48] and is expected to form upon ionization along with possible evaporation of neutral neon atoms.

B. Ionization of neon clusters doped with CO_2: Mass spectrum

Figure 2 shows the electron ionization mass spectra for neon clusters doped with CO_2 in the m/z range from 81–314. The electron energy used to measure this spectrum was 70 eV. The nozzle temperature was 80 K and the neon pressure 20 bar, i.e., the initial mean size of neon clusters was $\langle N \rangle \sim 45$. The pickup pressure in the chamber after the expansion chamber was 8×10^{-4} mbar. The mass resolution in this mass spectrum is lower than unit mass resolution. However, the low mass resolution led to a higher transmission of the quadrupole mass analyzer. Clearly visible is a series of peaks with decreasing intensity. The series in the shown mass range starts at m/z 88 and the following mass peaks are separated by 44 masses. Therefore, this peak series corresponds to the intact $(CO_2)_n^+$ cluster ions with $n = 2-7$. It should be noted that due to the low binding energy of the CO_2 molecules in a small CO_2 cluster, the neutral CO_2 cluster will shrink by the release of single CO_2 molecules upon ionization. The incremental binding energy (i.e., the energy released when one CO_2 unit is added to a CO_2 cluster of N molecules) increases from about 0.1 eV for $N = 3$ to about 0.19 eV for $N = 12$ [49]. In addition, also all residual neon is released from the cluster upon ionization, since almost no neon-containing cluster ions are observed—except for two ions which are labeled in the inset of Fig. 2. This inset shows the ion signals in the mass range between m/z 176[$(CO_2)_4^+$] and m/z 220[$(CO_2)_5^+$] in more detail. Although the mass resolution is limited, the spacing between the peaks is sufficient to allow an assigment. The three most abundant ones between the intact tetramer and pentamer cluster ion can be assigned to a fragmented CO_2 cluster, i.e., $(CO_2)_4O^+$ at m/z 192, $(CO_2)_4CO^+$ at m/z

204 and $(CO_2)_4O_2^+$ at m/z 208, respectively. Three previous electron ionization studies with bare CO_2 clusters reported these fragment ions in the mass spectrum at 70 eV as well [50–52]. Two of these studies [50,51] obtained a similar ratio of 1: ∼0.6: ∼0.3 for $(CO_2)_4O^+$: $(CO_2)_4CO^+$: $(CO_2)_4O_2^+$. In the present mass spectrum the ratio is 1: ∼0.7: ∼1.8, i.e., a considerable relative enhancement of $(CO_2)_4O_2^+$ can be obtained here. $(CO_2)_4O_2^+$ may form via two different fragmentation pathways: a one-step reaction with emission of a single carbon atom and a two-step reaction with the sequential loss of two CO units from different CO_2 molecules in a cluster. The latter reaction was suggested for bare clusters, since it is energetically more favorable [51]. Boatwright *et al.* studied electron ionization of helium nanodroplets doped with CO_2 [53]. In their mass spectrum at 70 eV, the $(CO_2)_nO_2^+$ was by far the dominant fragment ion and almost reached the abundance of the following intact cluster cation $(CO_2)_{n+1}^+$. Since the ionization of dopants in helium droplets mainly occurs via charge transfer from ionized He^+, they concluded that for this ionization mechanism the energy criterion is always fulfilled and direct carbon emission becomes the most probable channel [53]. The analogous explanation might be considered here, taking into account that the ionization energy of neon is only about 3 eV lower than that of helium. The data discussed in the next section shows that initial charge transfer from ionized neon is a dominant mechanism.

We also note that Heinbuch *et al.* studied soft x-ray ionization (at a photon energy of 26.5 eV) of bare CO_2 clusters [54] and observed only little fragmentation of the clusters upon ionization. For all studied cluster sizes they obtained a summed relative intensity for fragment ions of less than 0.01, which is much lower than for electron ionization. Therefore, it was concluded that nearly all excess energy above the ionization limit is removed by the photoelectron, and only a small part of the photon energy is deposited into the ionized cluster [54].

C. Ionization of neon clusters doped with CO_2: Appearance energies

In the course of present studies with doped neon clusters we also studied the electron ionization close to the threshold in order to investigate possible ionization mechanisms. The threshold behavior of $(CO_2)_4^+$ was measured for three different temperatures of the nozzle, i.e., different initial sizes of the neutral neon cluster. The neon pressure was kept at 20 bar for all measurements. The AE values of the thresholds observed are listed in Table II. Figure 3 shows the resulting ion yield measured at the nozzle temperature of 100 K ($\langle Ne \rangle = 21$). The ion yield indicates a first onset far below the ionization energy of neon. Using the fitting program based on PYTHON, we obtained an AE of 13.61 ± 0.09 eV for $(CO_2)_4^+$. This value is close to the ionization energy of the single CO_2 molecule. The NIST database [37] lists a range of values between 13.75 ± 0.05 eV [55] and 13.89 ± 0.03 eV [56] for the AE of the molecular cation formed by electron ionization. Appearance energies of cluster ions formed upon supersonic expansion of CO_2 gas with subsequent electron ionization of bare clusters were also reported previously. Stephan *et al.* reported

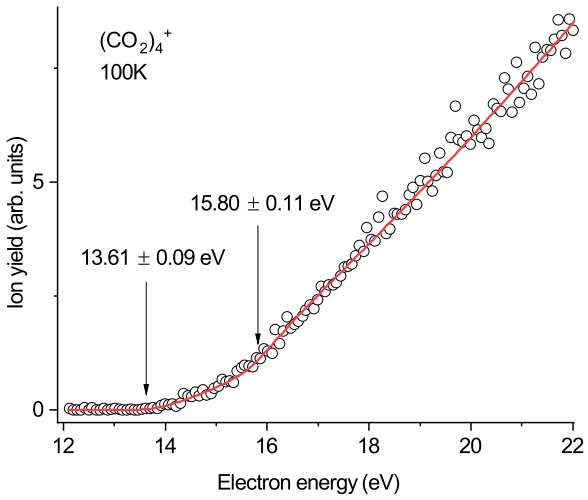

FIG. 3. Threshold ionization efficiency curve of $(CO_2)_4^+$ measured at the nozzle temperature of 100 K (open circles). The fit curve is shown as a solid line. The arrows indicate the derived thresholds.

the AE of 13.1 ± 0.2 eV [57]. This value is in agreement with the result from Cameron *et al.* [58], who reported the AE of 13.1 ± 0.1 eV. They also reported the AE for the tetramer and pentamer ion and obtained a gradual decrease of the AE with cluster size. They observed the AE $(CO_2)_4^+ = 12.6 \pm 0.1$ eV, which is about 1 eV lower than the present value. Analogously as suggested for rare gas clusters, Cameron *et al.* proposed that autoionization of Rydberg states leads to the observation that the AE of cluster ions is considerably lower than the ionization energy of the single molecule. In contrast, Klots and Compton mentioned in Ref. [59] that the AEs of the dimer and trimer ion of CO_2 are at a maximum 0.1 eV below the AE of the monomer and therefore they ruled out a strong cluster effect. The present measurement indicates the same tendency. We further note that the fit of the ion yield shown in Fig. 3 converged only if a second onset is assumed. This led to the appearance of a weakly abundant second threshold at 15.80 ± 0.11 eV. Since this value is still far lower than the lowest excitation energy of Ne (see below), we assign it to an excited state of CO_2. Bussieres and Marmet studied electron ionization of the CO_2 molecule [60] and derived a dip at about 15.5 eV in the ion efficiency curve of CO_2^+ by frequency filtering and smoothing the data. They assigned this dip to the threshold of Rydberg excitation of the neutral CO_2 molecule in competition to ionization. The existence of such Rydberg states was previously mentioned by Sanche and Schulz [61]. In the case of clusters, autoionization of this Rydberg state may be possible and will contribute to the ion yield. This may explain the observation of the second threshold in the present data.

Figure 4 shows the ion efficiency curve measured at a temperature of 75 K, corresponding to a mean cluster size of $\langle Ne \rangle = 60$. Compared to the measurement at 100 K, the signals below about 16 eV, corresponding to the ionization of a bare CO_2 cluster, represent a minor feature in the ion yield. A weak first threshold appears at 13.91 ± 0.09 eV, which can be assigned to direct ionization of the CO_2 cluster. Above this onset, the ion signal slowly raises until the second onset found at 16.60 ± 0.07 eV. Above this energy, the ion signal deviates from the Wannier-type ionization behavior and

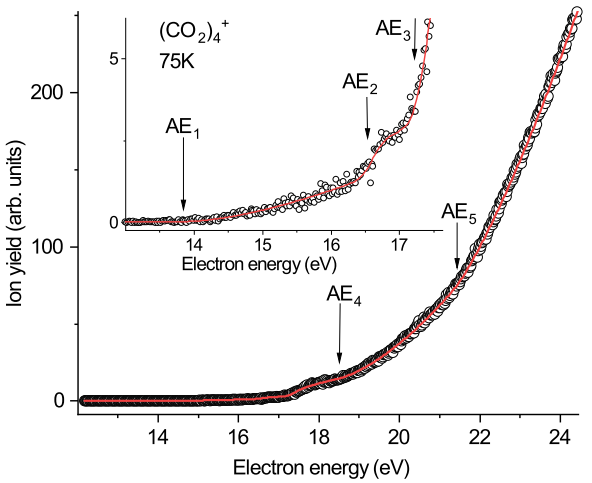

FIG. 4. Threshold ionization efficiency curve of $(CO_2)_4^+$ measured at the nozzle temperature of 75 K (open circles). The inset shows a more detailed view of the ion yield in the electron energy range between 13 and 17.6 eV. The fit curve is shown as a solid line. The arrows indicate the derived thresholds at $AE_1 = 13.91 \pm 0.09$ eV, $AE_2 = 16.60 \pm 0.07$ eV, $AE_3 = 17.31 \pm 0.02$ eV, $AE_4 = 18.5 \pm 0.1$ eV, and $AE_5 = 21.47 \pm 0.07$ eV.

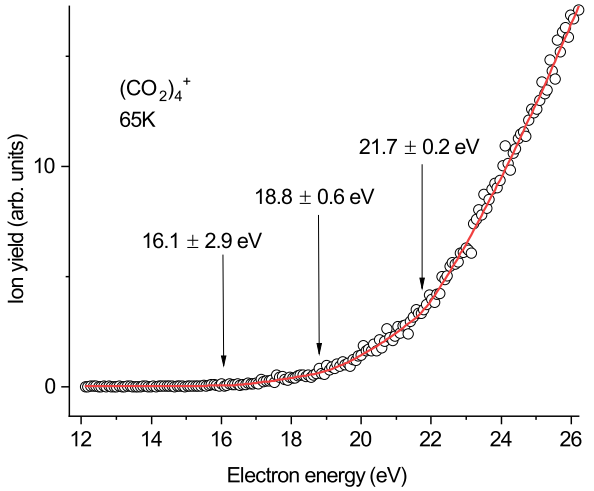

FIG. 5. Threshold ionization efficiency curve of $(CO_2)_4^+$ measured at the nozzle temperature of 65 K (open circles). The fit curve is shown as a solid line. The arrows indicate the derived thresholds.

instead shows a clear plateau at about 18 eV. Such features of the ion signal rather resemble the characteristic behavior of electronic excitation functions [62]. Therefore we propose that the ion yield forms by Penning ionization [63], where inelastic electron interaction with the mixed cluster leads first to the formation of a metastable neon atom Ne*. This electronically excited atom has sufficient energy to subsequently ionize the CO_2 cluster. The excitation function of neon is well known and has been reported in Refs. [64–66]. The onset of the energetically lowest metastable state $Ne^*(3s\,^3P_2)$, which has a lifetime of about 14.7 s [67], was experimentally found at 16.619 eV [68,69]. The presently observed onset at 16.60 ± 0.07 eV is in very good agreement with this value. Above the first onset, the excitation function also showed a series of Feshbach resonances, where the first one was located at 16.91 eV and another series of narrow resonances was found between 18.38 and 18.96 eV [66]. We note that the ion efficiency curve shown in Fig. 4 does not indicate any formation of a resonance, which is likely related to the short lifetime of these resonances in the order of $10^{-13}-10^{-14}$ s. However, above the first resonance the excitation function shows a dip at ∼17.2 eV before it raises again [64–66]. We note that we observe the third threshold at 17.31 ± 0.02 eV, which may result from the shape of the excitation function in this energy range. Following the mentioned plateau, we observe a fourth threshold at 18.5 ± 0.1 eV. Bömmels *et al.* [66] mentioned that the excitation function has contributions from $Ne^*(2p^5\,3s$ levels) above their lowest onset at 18.38 eV. Those states are short lived, but they decay to metastable states. Therefore, this cascade contribution may explain the presently observed fourth onset in the $(CO_2)_4^+$ ion yield. Finally, we observe a fifth onset at 21.47 ± 0.07 eV, as shown in Fig. 4. This onset can be ascribed to charge-transfer ionization of the CO_2 cluster, where initially a neon in the mixed cluster was ionized by the incoming electron and subsequently, the charge is transferred to the CO_2 dopant cluster.

The ionization mechanism involving charge transfer from ionized neon becomes also the dominant mechanism for larger neon clusters. Figure 5 shows the resulting curve measured for a nozzle temperature of 65 K ($\langle Ne \rangle = 143$). Notably, the $(CO_2)_4^+$ ion yield below the ionization energy of neon is only weak and the plateau observed at 75 K is diminished. Thresholds indicating a weak occurrence of Penning ionization are at 16.1 ± 2.9 and 18.8 ± 0.6 eV. These thresholds agree within the error with the onsets observed at 75 K. Since we do not observe a threshold corresponding to the ionization of bare CO_2 clusters, Penning ionization is the only ionization mechanism below the ionization energy of neon at these experimental conditions.

IV. CONCLUSION

In the present study we investigated electron ionization of bare neon clusters and neon clusters doped with CO_2 molecules. For the bare cluster ions Ne_n^+ (with $n = 2-6$), appearance energies have been derived which are only slightly lower than the ionization energy of the single neon atom. The presently obtained AE value of the dimer is 21.06 ± 0.07 eV and clearly exceeds the adiabatic ionization energy of 20.285 eV. An explanation for this deviation is most likely delivered from experiments varying the initial cluster size [9], since it turned out that the AE may become higher if the mean neutral cluster size is increased. In this case, the dimer ion is predominatly formed by dissociative electron ionization of larger clusters. The obtained similarity of the AE values for different cluster sizes—which are closer to the vertical ionization energy—support this explanation. In contrast, photoionization experiments are close to the adiabatic values as expected.

In the second part of our studies with neon clusters, we doped the clusters with CO_2 before electron ionization. By measuring the $(CO_2)_4^+$ ion yield as a function of the initial electron energy close to the threshold, it was possible to reveal different ionization mechanisms leading to the formation of $(CO_2)_4^+$. The derived AEs indicate that at rather warm

conditions of the cluster source (intial mean neon cluster size before pickup $\langle Ne \rangle = 21$) it was possible to generate bare CO_2 clusters by the pickup, which become directly ionized by an incoming electron. At intermediate conditions ($\langle Ne \rangle = 60$), the $(CO_2)_4^+$ forms upon Penning ionization by metastable Ne* above the thresholds of the corresponding excitations as well as charge-transfer ionization. The 70-eV mass spectrum at similar expansion conditions indicates that most residual neon becomes evaporated from all clusters after ionization. Finally, for the largest mean size studied, $\langle Ne \rangle = 143$, the $(CO_2)_4^+$ ion yield predominatly shows features from charge-transfer ionization, while the ion yield characteristic for metastable excitation functions below the ionization energy of neon is almost quenched. This transformation of the ion yield may also allow a conclusion on the localization of the dopant in the neon cluster. Slavicek *et al.* studied pickup and photodissociation of hydrogen halide in neon clusters for the size range $\langle Ne \rangle = 100-1600$ and concluded that in this size range, the dopant is fully buried in the neon matrix [70]. This result did not confirm the conclusions from fluorescence excitation spectroscopy studies by von Pietrowski *et al.* [21] who claimed a phase transition from fluid to solid at $N \geqslant 300$. Instead, Slavicek *et al.* proposed that a cluster with $N = 300$ has a solid core but still a liquid outer shell, while a neon cluster with $N = 130$ has a semiliquid core and a liquid surface. This situation would apply for the largest mean neon cluster size studied here, where we observe the signature of an interior state. For even smaller clusters, $\langle Ne \rangle = 60$, CO_2 states closer to the cluster surface become more relevant. This may manifest in the stronger contribution of Penning ionization.

ACKNOWLEDGMENTS

This work has been supported by the FWF, Wien, Austria (Contract No. P24443). R.M. acknowledges the Portuguese National Funding Agency FCT through PD/BD/114452/2016 and research grants UCIBIO (Grant No. UIDB/04378/2020) and CEFITEC (Grant No. UIDB/00068/2020). This work was also supported by Radiation Biology and Biophysics Doctoral Training Programme (RaBBiT, PD/00193/2012).

[1] A. Mauracher, O. Echt, A. M. Ellis, S. Yang, D. K. Bohme, J. Postler, A. Kaiser, S. Denifl, and P. Scheier, Phys. Rep. **751**, 1 (2018).
[2] M. Gatchell, P. Martini, L. Kranabetter, B. Rasul, and P. Scheier, Phys. Rev. A **98**, 022519 (2018).
[3] T. D. Märk and P. Scheier, Chem. Phys. Lett. **137**, 245 (1987).
[4] P. Scheier and T. D. Märk, J. Chem. Phys. **87**, 5238 (1987).
[5] M. J. DeLuca, D. M. Cyr, W. A. Chupka, and M. A. Johnson, J. Chem. Phys. **92**, 7349 (1990).
[6] M. Fieber, G. Bröker, and A. Ding, Z. Phys. D: At. Mol. Clusters **20**, 21 (1991).
[7] I. Mähr, F. Zappa, S. Denifl, D. Kubala, O. Echt, T. D. Märk, and P. Scheier, Phys. Rev. Lett. **98**, 023401 (2007).
[8] S. Denifl, M. Stano, A. Stamatovic, P. Scheier, and T. D. Märk, J. Chem. Phys. **124**, 054320 (2006).
[9] O. Echt, T. Fiegele, M. Rümmele, M. Probst, S. Matt-Leubner, J. Urban, P. Mach, J. Leszczynski, P. Scheier, and T. D. Märk, J. Chem. Phys. **123**, 084313 (2005).
[10] M. Lewerenz, B. Schilling, and J. P. Toennies, J. Chem. Phys. **102**, 8191 (1995).
[11] F. Ancilotto, P. B. Lerner, and M. W. Cole, J. Low Temp. Phys. **101**, 1123 (1995).
[12] C. E. Klots, Nature (London) **327**, 222 (1987).
[13] M. A. Gaveau, M. Briant, P. R. Fournier, J. M. Mestdagh, and J. P. Visticot, J. Chem. Phys. **116**, 955 (2002).
[14] M. Dvorak, M. Müller, T. Knoblauch, O. Bünermann, A. Rydlo, S. Minniberger, W. Harbich, and F. Stienkemeier, J. Chem. Phys. **137**, 164301 (2012).
[15] O. Stauffert, S. Izadnia, F. Stienkemeier, and M. Walter, J. Chem. Phys. **150**, 244703 (2019).
[16] M. Dvorak, M. Müller, T. Knoblauch, O. Bünermann, A. Rydlo, S. Minniberger, W. Harbich, and F. Stienkemeier, J. Chem. Phys. **137**, 164302 (2012).
[17] M. A. Gaveau, M. Briant, P. R. Fournier, J. M. Mestdagh, and J. P. Visticot, Phys. Chem. Chem. Phys. **2**, 831 (2000).
[18] R. Baumfalk, N. Hendrik Nahler, and U. Buck, Faraday Discuss. **118**, 247 (2001).
[19] F. Marinetti and F. A. Gianturco, Phys. Chem. Chem. Phys. **13**, 2136 (2011).
[20] M. Müller, S. Izadnia, S. M. Vlaming, A. Eisfeld, A. LaForge, and F. Stienkemeier, Phys. Rev. B **92**, 121408(R) (2015).
[21] R. von Pietrowski, K. von Haeften, T. Laarmann, T. Möller, L. Museur, and A. V. Kanaev, Eur. Phys. J. D **38**, 323 (2006).
[22] R. Baumfalk, N. H. Nahler, U. Buck, M. Y. Niv, and R. B. Gerber, J. Chem. Phys. **113**, 329 (2000).
[23] F. Calvo, F. Spiegelman, and M.-C. Heitz, J. Chem. Phys. **118**, 8739 (2003).
[24] M. Briant, M. A. Gaveau, P. R. Fournier, J. M. Mestdagh, J. P. Visticot, and B. Soep, Faraday Discuss. **118**, 209 (2001).
[25] M.-A. Gaveau, E. Gloaguen, P.-R. Fournier, and J.-M. Mestdagh, J. Phys. Chem. A **109**, 9494 (2005).
[26] S. Denifl, F. Zappa, I. Mähr, A. Mauracher, M. Probst, J. Urban, P. Mach, A. Bacher, D. K. Bohme, O. Echt, T. D. Märk, and P. Scheier, J. Chem. Phys. **132**, 234307 (2010).
[27] D. Bonhommeau, P. T. Lake, C. Le Quiniou, M. Lewerenz, and N. Halberstadt, J. Chem. Phys. **126**, 051104 (2007).
[28] E. Jabbour Al Maalouf, M. Neustetter, E. Illenberger, P. Scheier, and S. Denifl, J. Phys. Chem. Lett. **8**, 2220 (2017).
[29] U. Buck and R. Krohne, J. Chem. Phys. **105**, 5408 (1996).
[30] B. Gstir, S. Denifl, G. Hanel, M. Rümmele, T. Fiegele, P. Cicman, M. Stano, S. Matejcik, P. Scheier, K. Becker, A. Stamatovic, and T. D. Märk, J. Phys. B: At., Mol. Opt. Phys. **35**, 2993 (2002).
[31] G. Hanel, B. Gstir, T. Fiegele, F. Hagelberg, K. Becker, P. Scheier, A. Snegursky, and T. D. Märk, J. Chem. Phys. **116**, 2456 (2002).
[32] M. Stano, S. Matejcik, J. D. Skalny, and T. D. Märk, J. Phys. B: At., Mol. Opt. Phys. **36**, 261 (2003).
[33] G. H. Wannier, Phys. Rev. **90**, 817 (1953).

[34] S. Denifl, S. Matejčík, J. D. Skalný, M. Stano, P. Mach, J. Urban, P. Scheier, T. D. Märk, and W. Barszczewska, Chem. Phys. Lett. **402**, 80 (2005).
[35] R. Meißner, L. Feketeová, A. Bayer, J. Postler, P. Limão-Vieira, and S. Denifl, J. Mass Spectrom. **54**, 802 (2019).
[36] M. Renzler, M. Daxner, N. Weinberger, S. Denifl, P. Scheier, and O. Echt, Phys. Chem. Chem. Phys. **16**, 22466 (2014).
[37] *NIST Chemistry WebBook, NIST Standard Reference Database Number 69*, edited by P. J. Linstrom and W. G. Mallard (National Institute of Standards and Technology, Gaithersburg, MD, USA).
[38] N. Moiseyev, R. Santra, J. Zobeley, and L. S. Cederbaum, J. Chem. Phys. **114**, 7351 (2001).
[39] T. Van Mourik, A. K. Wilson, and T. H. Dunning, Mol. Phys. **96**, 529 (1999).
[40] J. Masik, J. Urban, P. Mach, and I. Hubac, Int. J. Quantum Chem. **63**, 333 (1997).
[41] T. Fiegele, Ph.D. thesis, University of Innsbruck, 2001.
[42] M. S. B. Munson, J. L. Franklin, and F. H. Field, J. Phys. Chem. **67**, 1542 (1963).
[43] R. I. Hall, Y. Lu, Y. Morioka, T. Matsui, T. Tanaka, H. Yoshii, T. Hayaishi, and K. Ito, J. Phys. B: At., Mol. Opt. Phys. **28**, 2435 (1995).
[44] D. J. Trevor, J. E. Pollard, W. D. Brewer, S. H. Southworth, C. M. Truesdale, D. A. Shirley, and Y. T. Lee, J. Chem. Phys. **80**, 6083 (1984).
[45] E. C. M. Chen, J. G. Dojahn, and W. E. Wentworth, J. Phys. Chem. A **101**, 3088 (1997).
[46] P. Svrčkov, A. Vtek, F. Karlick, I. Paidarov, and R. Kalus, J. Chem. Phys. **134**, 224310 (2011).
[47] F. Calvo, F. Y. Naumkin, and D. J. Wales, Chem. Phys. Lett. **551**, 38 (2012).
[48] F. Sebastianelli, E. Yurtsever, and F. A. Gianturco, Int. J. Mass Spectrom. **220**, 193 (2002).
[49] J. Norooz Oliaee, M. Dehghany, A. R. W. McKellar, and N. Moazzen-Ahmadi, J. Chem. Phys. **135**, 044315 (2011).
[50] A. Stamatovic, K. Stephan, and T. D. Märk, Int. J. Mass Spectrom. Ion Processes **63**, 37 (1985).
[51] G. Romanowski and K. P. Wanczek, Int. J. Mass Spectrom. Ion Processes **62**, 277 (1984).
[52] J. Dąbek and L. Michalak, Vacuum **63**, 555 (2001).
[53] A. Boatwright, J. Jeffs, and A. J. Stace, J. Phys. Chem. A **111**, 7481 (2007).
[54] S. Heinbuch, F. Dong, J. J. Rocca, and E. R. Bernstein, J. Chem. Phys. **125**, 154316 (2006).
[55] J.-D. Carette, Can. J. Phys. **45**, 2931 (1967).
[56] V. E. Sahini, V. Constantin, and I. Serban, Rev. Roum. Chim. **23**, 479 (1978).
[57] K. Stephan, T. Märk, J. Futrell, and A. Castleman, Vacuum **33**, 77 (1983).
[58] B. R. Cameron, C. G. Aitken, and P. W. Harland, J. Chem. Soc. Faraday Trans. **90**, 935 (1994).
[59] C. E. Klots and R. N. Compton, J. Chem. Phys. **67**, 1779 (1977).
[60] N. Bussieres and P. Marmet, Can. J. Phys. **55**, 1889 (1977).
[61] L. Sanche and G. J. Schulz, J. Chem. Phys. **58**, 479 (1973).
[62] M. Danko, A. Ribar, M. Ďurian, J. Országh, and Š. Matejčík, Plasma Sources Sci. Technol. **25**, 065007 (2016).
[63] S. Falcinelli, P. Candori, M. Bettoni, F. Pirani, and F. Vecchiocattivi, J. Phys. Chem. A **118**, 6501 (2014).
[64] J. N. H. Brunt, G. C. King, and F. H. Read, J. Phys. B: At., Mol. Phys. **9**, 2195 (1976).
[65] S. J. Buckman, P. Hammond, G. C. King, and F. H. Read, J. Phys. B: At., Mol. Phys. **16**, 4219 (1983).
[66] J. Bömmels, K. Franz, T. H. Hoffmann, A. Gopalan, O. Zatsarinny, K. Bartschat, M. W. Ruf, and H. Hotop, Phys. Rev. A **71**, 012704 (2005).
[67] M. Zinner, P. Spoden, T. Kraemer, G. Birkl, and W. Ertmer, Phys. Rev. A **67**, 010501(R) (2003).
[68] M. Allan, K. Franz, H. Hotop, O. Zatsarinny, and K. Bartschat, J. Phys. B: At., Mol. Opt. Phys. **42**, 044009 (2009).
[69] O. Zatsarinny and K. Bartschat, Phys. Rev. A **86**, 022717 (2012).
[70] P. Slavíček, P. Jungwirth, M. Lewerenz, N. H. Nahler, M. Fárník, and U. Buck, J. Phys. Chem. A **107**, 7743 (2003).